International Journal of Research in Advent Technology, Special Issue, March 2019
E-ISSN: 2321-9637
3rd National Conference on Recent Trends & Innovations In Mechanical Engineering

15th & 16th March 2019

Available online at www.ijrat.org

Effect Of Heat Input On Weld Defects Using X-Ray Radiography

Yelamasetti Balram[1], T Vishnu Vardhan[2], G Venkata Ramana[3], B Sridhar Babu[4], Harinadh Vemanaboina[5],

[1,2,3,4] CMR Institute of Technology, Kandlakoya, Medchal, Telangana-501401, India.

Nalla Narasimha Reddy Education Society's Group of Institutions, Ghatkesar, Ranga Reddy- 500088, India.

Abstract: Non-Destructive Testing (NDT) of welded structures plays a key role in ensuring the reliable performance of weld structures. In this study, the quality of the dissimilar weldments of AISI 316 and Monel 400 was evaluated by employing X-Ray radiography technique. For joining these weldments Gas Tungsten Arc Welding (GTAW) process has been employed. The quality of the welded structures mainly depends on total heat input rates given to the base metals. The effect of welding current on quality of welded structure was reported. Due to the lack of fusion in sample ID-(a) the weld defect was observed.
Keywords: Dissimilar joints, GTAW process, Welding current, X-Ray Radiography test.

1. INTRODUCTION

Quality of welded structures allow to provide industry satisfaction and reduce the danger and cost of changing wrong products. Mostly, the inspection of structures should be done very accurate before it is delivered to industry. NDT technology plays an important role in ensuring the performance of the welded structures [1]. The commonly used NDT methods are radiography, magnetic resonance imaging, and ultrasonic imaging. These NDT methods are used to inspect the defects and discontinuities. The X-ray Radiography Testing (X-RT) is employed in many manufacturing industries to ascertain the weld quality by assessing the radiographs of the welded structures by an expert operator [2]. In this technique, the X-rays or γ- rays are used to penetrate a weldment and detect any defects or discontinuities present in welded structures [3]. The X-rays are used to inspect the thin as well as thick weld defects such as cracks, micro-porous, discontinuities and voids [4].

The Ni-Cu type alloys, such as Monel 400, generally solidify as single-phase austenite with no secondary constituents. This is to be expected based on the simple Ni-Cu isomorphous phase structure that exhibits complete solid solubility across the entire composition range [5]. Monel 400 exhibits excellent fatigue strength and good ductility along with corrosion resistance at elevated temperature. Similarly, austenitic stainless steels are Iron-based alloys, having good toughness, ductility and excellent resistance at high temperatures, and they are often referred as heat-resisting alloys [6]. These types of applications are most often found in nuclear, petrochemical and marine applications where the welds are usually exposed to higher temperatures [7].

Fusion welding process widely used in nuclear, petrochemical industries and air craft's applications due to easy setup and low cost [8]. GTAW process which uses an argon gas for shielding and tungsten electrode for welding torch for joining hard materials like steel grades, Ni-based alloys etc. [9, 10]. The high amount of heat is produced during welding process which effects the quality of the welded structures. The quality of the welded structure mainly depends on welding current, arc voltage and gas flow rate [11].

In this study, three levels of welding currents have been selected for evaluating the quality of the weldments. The arc voltage and gas flow rate are considered as constant. Here, CEREM 235 Radiography machine has been employed to inspect the weldments of AISI 316 and Monel 400.

2. EXPERIMENTATIONS

2.1 Materials And Welding Procedure

The base metals, AISI 316 and Monel 400 plates of (120 mm x 60 mm x 5 mm) dimension are considered for V groove configuration. The groove configuration of welds is shown in Fig. 1. Ni-based filler wire ERNiCrMo-3 was chosen as it is suitable for both the base metals in terms of phase structures and chemical composition [12]. The chemical composition in wt.% shown in Table 1. For joining these base metals GTA welding process has been employed. The process parameters of GTAW process are listed in Table.2. Before joining of base materials, tack welding process is made to avoid the misalignment and for maintaining a constant root gap between both the base materials. These base metals were clamped firmly in the fixture designed with a steel back plate so as to reduce bending and distortions during welding process. During welding, argon shielding gas with a flow rate of 10 lpm was used to prevent the oxidation of the base and weldments. For filling 5 mm base plates the multi-pass (3 pass) welding process has been performed to produce good welds. The heat input to the base metals has been calculated by using equation (1). The developed weldments are shown in Fig. 2.

$$\text{Efficiency of heat source } (\eta) = \frac{Energy\ transferred\ to\ the\ workpiece\ (Q)}{Energy\ generated\ by\ the\ heat\ source}$$

$$Q_{GTAW} = \eta V * I \quad kJ \qquad (1)$$

Table 1. Chemical composition in %wt. filler and base metals

Filler metal/ base	Ni	Fe	Cu	Cr	Mn	C	Mo	Si	Others
ERNiCrMo-3	Rem	5.0	0.5	21.5	0.5	0.1	9.0	0.5	Co-9.0, Nb-3, Ti-0.4
Monel 400	Rem	2.5	31.5	---	1.6	0.12	---	0.4	----
SS 316	10.4	Rem	---	17.9	2.0	0.08	2.1	0.4	P- 0.002

Table 2. Process parameters for GTAW process

Sample ID	Current (I), A	Voltage (V), V	Efficiency (η)	Heat input (Q), kJ
A	120	14	0.7	1176
B	130	14	0.7	1274
C	140	14	0.7	1372

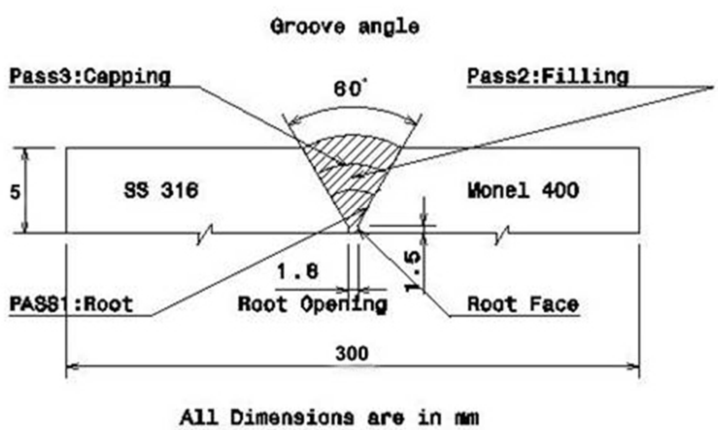

Fig. 1. Schematic diagram of weld groove design

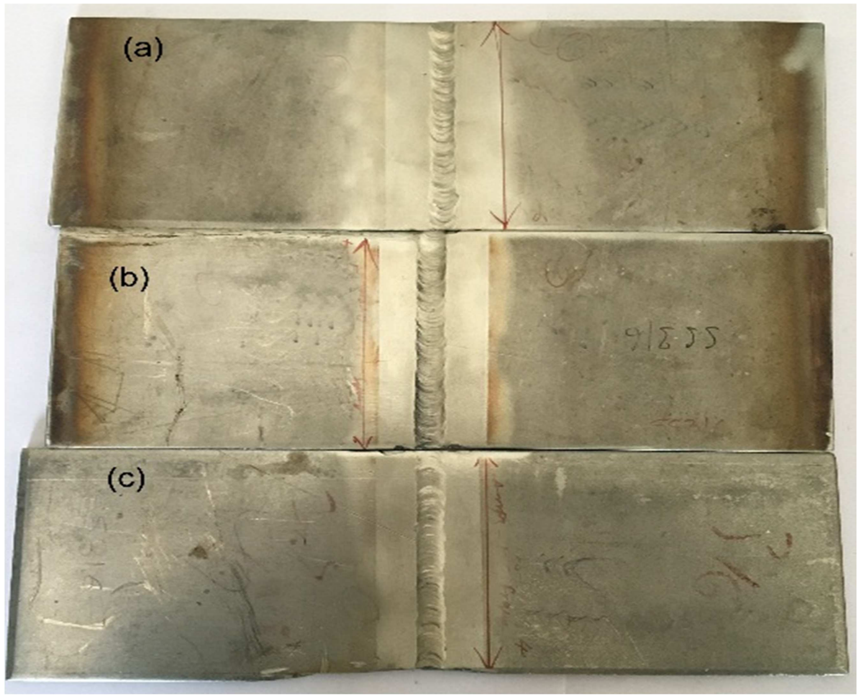

Fig. 2. Dissimilar welded joints of AISI 316 and Monel 400

2.2 X-Ray Radiography Test

X-rays are produced when high speed electrons, in the form of a beam called cathode ray, strike a metal target placed in an X-ray tube. The velocity at which the electrons strike the target is determined by the tube voltage where the tube voltage is the potential difference between the source. The X-rays are allowed to fall upon the test specimen. Some of the X-rays are absorbed. The extent of this absorption, as already stated earlier, depends on the presence of voids, foreign inclusions, or cracks in the weld metal. As a result, the radiation passing through the weld and falling upon a photographic plate or film behind it will produce areas differing in optical density, dark spots corresponding to denser areas and light spots to some defects in the inferior of the weld. The quality of the resulting picture depends on the intensity of the radiation source, the angle of inclination of the X-rays, the type and thickness of metal.

In this study, CEREM 235 Radiography testing machine was used for reviewing internal defects in welded joints of dissimilar metals, AISI 316 and Monel 400. The welded joints were characterized for determining any micro/macroscopic defects using XRT according to American Society of Mechanical Engineers (ASME) SEC-8 standard. The X-ray source was used to observe the welded joints of wavelength and with an exposure time of 120 s. The main source voltage of 180 keV and a current of 3.5 mA were maintained.

3. RESULTS AND DISCUSSIONS

From the NDT analysis, the X-ray radiography images are free from macro defects are shown in Figs. 3, 4 and 5. From the Fig. 3, it is clearly indicated that linear crack (micro defect) on the weld bead geometry at 120 A welding current. In sample ID-a, the defect was identified wherein the welds are obtained with the lower heat input rates. Figs. 4 and 5 shows the radiographic films of welding current 130 A and 140 A. From these films, it can be clearly observed that the welds are free from discontinuities and defects. Whereas Fig. 4 shows the uniform welds are obtained at welding current of 130 A. The welding current 130 and 140 A are most suitable for joining dissimilar metals AISI 316 and Monel 400 when GTAW process is employed.

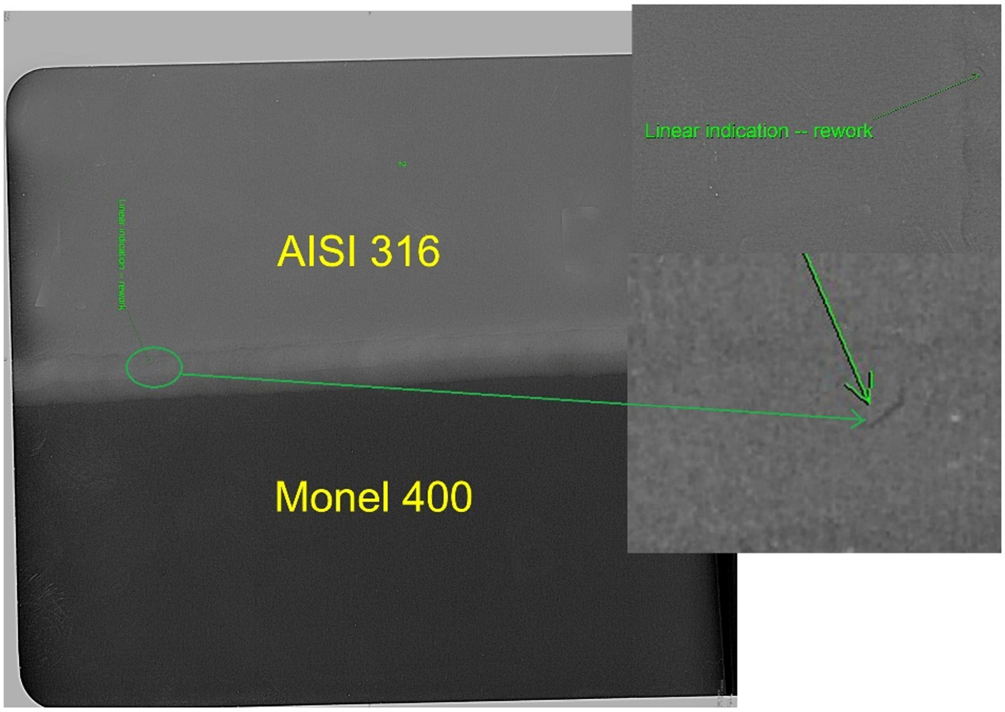

Fig. 3. X-Ray radiography image of Sample ID-(a)

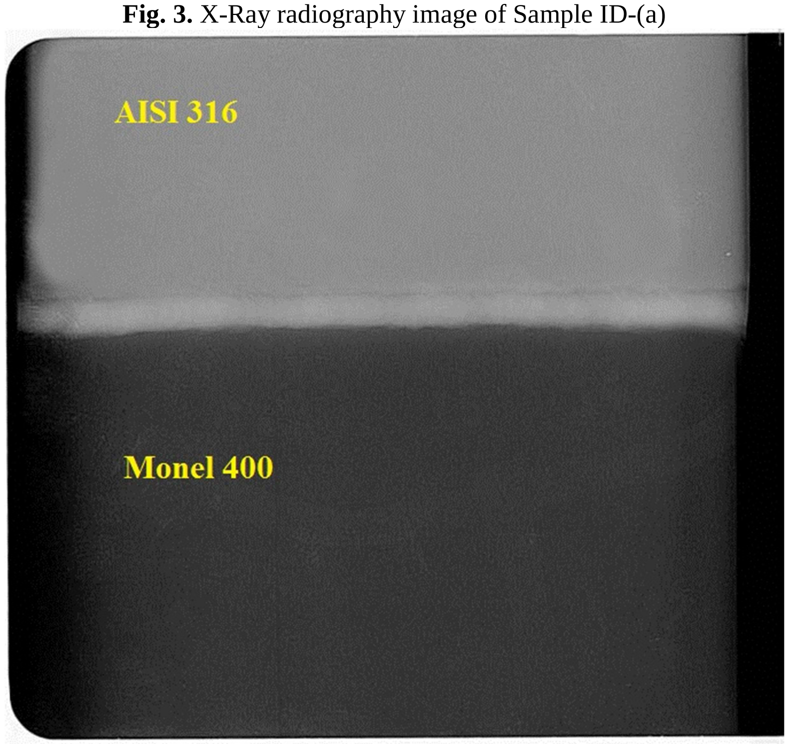

Fig. 4. X-Ray radiography image of Sample ID-(b)

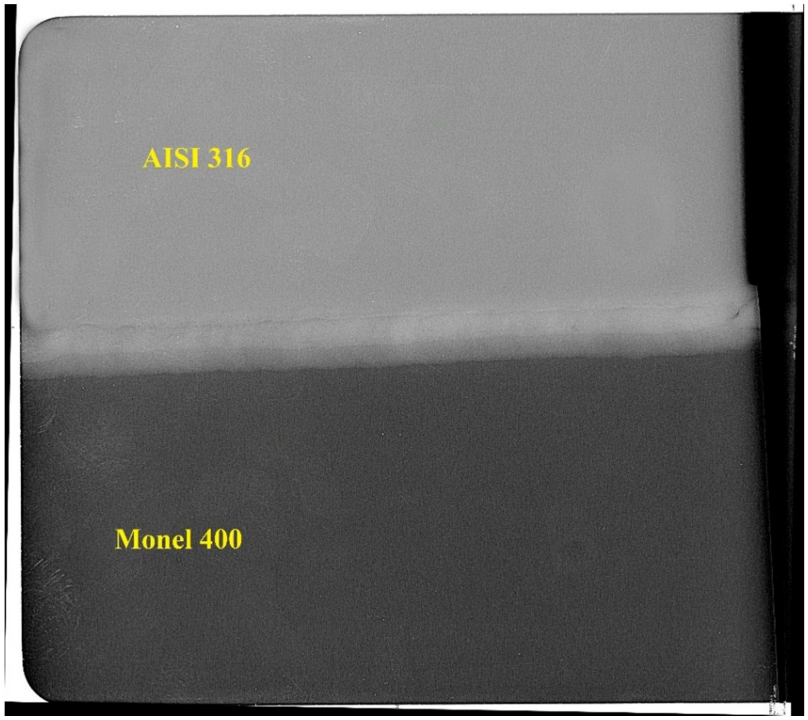

Fig. 5. X-Ray radiography image of Sample ID-(c)

4. CONCLUSIONS

The following conclusions are made from the experimental study of GTA welding process.

- Visual inspection test was successfully conducted on the welded joints of AISI 316 and Monel 400. Defect free welds were observed from the visual inspection for all the selected parameters and uniform weld is obtained at 130 A.
- The X-ray radiography test was performed successfully to detect the defect free weldments. Welds surfaces are free from defects on welds obtained at 130 A and 140 A.
- Linear defect was observed on the welds obtained at 120 A.

REFERENCES

[1] *R. S. Parmer*, Welding Engineering and Technology, second edition, Khanna Publishers, 2016.

[2] Yenumula L, Acharya R V., Lingade BM, Borgohain A, Maheshwari NK, Kumar U, et al. Radiographic evaluation of gas tungsten arc welded joints used in nuclear applications by X- and gamma-rays. NDT E Int 2019;102:144–52. doi:10.1016/j.ndteint.2018.11.017.

[3] Zahran O, Kasban H, El-Kordy M, El-Samie FEA. Automatic weld defect identification from radiographic images. NDT E Int 2013;57:26–35. doi:10.1016/j.ndteint.2012.11.005.

[4] Rathinasuriyan C, Senthil Kumar VS, Shanbhag AG. Radiography and corrosion analysis of sub-merged Friction Stir Welding of AA6061-T6 alloy. Procedia Eng 2014;97:810–8. doi:10.1016/j.proeng.2014.12.355.

[5] C.Lippold JND& J. Welding Metallurgy and Weldability of Nickel-Base Alloys. vol. 53. 2009. doi:10.1017/CBO9781107415324.004.

[6] John C. Lippold, Damian J. Kotecki-Welding Metallurgy and Weldability of Stainless Steels -Wiley-Interscience (2005) n.d.

[7] Yelamsetti B, Stresses R, Welds S, Welds D. THERMAL STRESS ANALYSIS OF SIMILAR AND DISSIMILAR WELDED

JOINTS 2018;80.

[8] Staple B. Welding Handbook Volume 4 Metals and Their Weldability. vol. 4. 1997.

[9] Hand book on Stainless Steel Welding C entre 2012.

[10] Vemanaboina H, Edison G, Akella S, Buddu RK. Effect of Residual Stresses of GTA Welding for Dissimilar Materials. Mater Res 2018;21. doi:10.1590/1980-5373-mr-2017-1053.

[11] Juang SC, Tarng YS. Process parameter selection for optimizing the weld pool geometry in the tungsten inert gas welding of stainless steel. J Mater Process Technol 2002;122:33–7. doi:10.1016/S0924-0136(02)00021-3.

[12] Davis JR. ASM Specialty Handbook: Nickel, Cobalt, and Their Alloys. 2000. doi:10.1361/ncta2000p013.